

Article

A BIM-Based Approach for Assessing Occupational Health Risks in a Building Construction Project

Apurva Jangam ¹, Daniel Cheriyan ² and Jae-Ho Choi ^{1,*}

¹ ICT Integrated Safety Ocean Smart Cities Engineering Department, Dong-A University, S12-401, 550 Bungil 37, Nakdong-Daero, Saha-Gu, Busan 49315, Republic of Korea; 2172329@donga.ac.kr

² John Molson School of Business, Concordia University, Montreal, QC H3G 1M8, Canada; danielcheriyan21@gmail.com

* Correspondence: jaehochoi@dau.ac.kr

Abstract: Construction work sites and the surrounding built environments are notable contributors to atmosphere dust particulate matter (PM) emissions. PM produced in construction processes contain a range of chemically hazardous substances, posing significant health risks (HR) to individuals. As such, the evaluation of occupational HR in construction has become a focal point of interest internationally. Initiated in the early 2000s, there has been a growing demand within the construction research community for the creation of a unified PM database that encapsulates a wide array of construction activities. Previous studies have endeavored to establish a PM database for various construction contexts, yet they have fallen short in thoroughly addressing the diversity of construction materials and the levels of toxic substances (TS) within the PM. This research introduced a comprehensive PM and TS dataset and conducted a case study to measure the HR associated with diverse construction processes. This was accomplished by implementing a semi-automated Building Information Modeling (BIM) version 2020-based plugin, which streamlines the assessment of occupational HR in construction projects. This system provides construction supervisors with a tool to visually assess the HR of daily operations, thereby facilitating the adoption of preemptive measures to protect the health of construction workers.

Keywords: particulate matter; toxic substance; HR index; BIM; PM control measures



Citation: Jangam, A.; Cheriyan, D.; Choi, J.-H. A BIM-Based Approach for Assessing Occupational Health Risks in a Building Construction Project. *Buildings* **2024**, *14*, 476. <https://doi.org/10.3390/buildings14020476>

Academic Editor: Irem Dikmen

Received: 11 December 2023

Revised: 23 January 2024

Accepted: 28 January 2024

Published: 8 February 2024



Copyright: © 2024 by the authors. Licensee MDPI, Basel, Switzerland. This article is an open access article distributed under the terms and conditions of the Creative Commons Attribution (CC BY) license (<https://creativecommons.org/licenses/by/4.0/>).

1. Introduction

The construction industry is a cornerstone of societal progress in building infrastructure. Yet, amidst its pivotal contributions, it also poses as a major environmental pollutant. This sector is responsible for approximately 70–80% of the total particulate matter (PM) emissions into the atmosphere [1,2]. The ramifications of this issue are concerning for the health of construction workers who are regularly exposed to construction-related dust. This exposure carries both short-term and long-term health risks (HRs), contributing to health issues within this labor-intensive field [3]. The challenges are aggravated by the demographic trend of an aging workforce in the construction industry. This risk is more pronounced in construction than in other industries like automotive manufacturing, biomass combustion, and power generation [2].

Despite considerable advancements in occupational health and safety, the construction sector continues to grapple with significant HRs [4]. Research has identified common construction activities such as drilling, cutting, sanding, and mixing as the primary culprits in PM emissions [5]. These activities, integral to construction processes, inadvertently contribute to the elevated levels of airborne particulates.

The health implications of PM exposure are extensive and varied. Diseases like asthma, cardiovascular disorders, silicosis, lung cancer, and other pulmonary conditions have been directly associated with PM exposure [6]. The complex chemical makeup of PM, consisting

of elements such as aluminum (Al), chlorine (Cl), iron (Fe), magnesium (Mg), potassium (K), sulfur (S), silicon (Si), lead (Pb), cadmium (Cd), zinc (Zn), and copper (Cu), has been underscored in various studies [6–8] as a significant HR. For instance, overexposure to lead can result in adverse effects on the nervous, skeletal, endocrine, and immune systems [9]. Similarly, excessive inhalation of copper is known to be linked with severe respiratory conditions, including chronic bronchitis, asthma, and lung cancer [10,11].

While numerous studies [1,4,6,7] have endeavored to evaluate and mitigate the HRs associated with PM and toxic substances (TSs), achieving precision in these investigations remains a challenge. For example, traditional land-based PM HR assessments [3] concluded the uniform PM concentration across construction sites. This assumption oversimplifies the complexity of the environment and overlooks the necessity of activity-specific HR evaluations. More recent research has begun to address this gap by considering different construction activities to gather more accurate PM HR emission data. Nonetheless, these studies frequently neglect the impact of varied construction materials and TSs on the HR [11]. For example, Li et al.'s [6] approach, which examined dust exposure across 33 construction sites and assessed only one material type per sample, differs from the simulation findings of Cheriyan et al. [12]. The latter study illustrated that PM emissions could exhibit significant variation based on the specific construction materials employed.

The increasing awareness among researchers since the early 2000s underscores the necessity of a unified PM emission dataset within the construction sector. This dataset is crucial for a thorough analysis and effective mitigation of health impacts linked to PM and TS exposure [11]. While previous studies [13,14] conducted simulations involving various activities and materials, the raw data from these simulations poses challenges in estimating the HRs. Recognizing this need and research gap, our primary objectives include standardizing the PM and TS emission exposure dataset from previous studies, introducing a robust Health Risk Index (HRI) based on a model recommended by the U.S. Environmental Protection Agency (USEPA) and lastly, streamlining HRI implementation. Additionally, we aim to introduce control measures related to HRs through a specialized Revit plugin. Leveraging the advanced technological capabilities of Building Information Modeling (BIM) version 2020, with its high visualization potential and widespread application in the construction industry [15,16], this plugin is designed to enhance the health management of workers involved in construction projects. This comprehensive initiative empowers construction managers to accurately calculate the HRs associated with diverse construction activities and implement effective control measures.

2. Literature Review

2.1. Occupational HR Assessment of PM and TSs in the Construction Industry

Increasing awareness of the HRs associated with exposure to PM and TSs in construction activities is evident in recent studies. A select group of researchers [3,8,17] have delved into HR assessments specific to construction, forging a deeper understanding of the link between HRs and pollutants produced by these activities. This section navigates through some literature, unraveling the key findings and insights garnered by researchers who have delved into the complex interplay between construction activities and health hazards.

De Moraes et al. [18] undertook an empirical study across five building sites, scrutinizing PM and total suspended particles (TSP) emissions emanating from concrete and masonry work. This study sheds light on the characteristics and composition of PM at construction sites, including the impact of meteorological variables and construction activities on PM concentration, while also acknowledging the limitations inherent in the research.

In another significant study, Latif et al. [5] assessed the exposure to various TSs during renovation tasks like demolition, drilling, sanding, cutting, and painting in a controlled laboratory setting. Here, PM₁₀ concentrations were observed to surpass the dust limit set by the Malaysian Department of Safety and Health (DOSH) in indoor environments (0.150 mg/m³), ranging from 0.166 mg/m³ to 0.542 mg/m³. Four TSs (Pb, Cd, Zn, and Cu) were identified, with Zn being the most prevalent, followed by Cu, Pb, and Cd. These

findings are attributed to the composition of the building materials and furnishings used during the renovation.

Tong et al. [19] explored the impact of construction dust on worker health across five different zones during the superstructure construction stage of residential projects in Beijing. Utilizing the USEPA risk assessment model, the Monte Carlo method, and a probabilistic risk assessment model, the study estimated the HRs attributable to construction dust, pinpointing the most significant parameters. The results indicated varying levels of construction dust-induced HRs across zones, in the order of template zone > steel zone > concrete area > floor zone > office zone. The study highlighted the elevated HR in the template zone, emphasizing the need for effective control measures to mitigate the adverse health effects of construction dust.

In summary, recent scholarly discourse demonstrates a growing awareness of HRs associated with exposure to PM and TSs in construction activities. The examination of HRs linked to TSs in this context remains limited. Furthermore, to achieve a comprehensive HR assessment, it is essential to integrate detailed information concerning the specific types of activities and materials involved in construction processes.

2.2. PM and TSs Database from Previous Studies

In response to the escalating awareness of occupational health hazards in the construction industry, recent studies have delved into assessing the risks associated with PM and TSs generated during construction activities. One such notable contribution is the work conducted by Choi et al. [14], where a meticulous evaluation was performed using the USEPA equation, incorporating real-time inhalation rate (IR) measurements. This research aimed to address the gaps in existing studies by implementing a focused approach on PM particles and conducting methodical experimental simulations. A series of methodical experimental simulations were conducted to assess the HR linked to various construction activities and materials. This research built upon the experimental framework outlined by Cheriyan et al. [20], with a focused revision towards prioritizing PM₁₀ particles. Monitoring stations were strategically placed one meter from the PM source to facilitate construction operations while ensuring accurate data collection. The experiments were executed within a dust chamber measuring $4 \times 4 \times 2.35 \text{ m}^3$, featuring walls and floors lined with adhesive mats that were moistened to reduce particle deflection.

The partition wall and sensors were positioned one meter apart, with a $3 \times 0.7 \text{ m}^2$ observation window facilitating external monitoring of the experiments. Activities typical of a construction setting, such as cutting, drilling, mixing, sanding, and plastering, were simulated using materials like wood, hollow blocks, solid blocks, and M20 and M25 grade substances. To account for PM particle settling time, each activity was spaced with a 24 h interval, and baseline levels were reassessed at similar intervals. If the PM levels exceeded the reference threshold, the experiment was deferred to the next day. The PM concentrations emitted during these activities were meticulously monitored, alongside fluctuations in the IR of construction workers. Data were systematically collected and stored using a computer, with results adapted and revised from Cheriyan et al. [20], as delineated in Tables 1 and 2. These tables provide a comprehensive overview of the PM concentrations during cutting, drilling, mixing, plastering, and sanding highlighting the variations in PM sizes and concentrations across different materials.

Given the unavailability of real-time TS monitoring equipment, this study embraced the gravimetric sampling methodology recommended by Khamraev et al. [21] for estimating real-time TS levels. PM collection was also executed using the MiniVol device [22] to ascertain the composition of TSs in various activities. During the solid block cutting, real-time (Alphasense OPC-N3) PM monitoring and gravimetric samplers were deployed concurrently. The diverse TSs were identified by analyzing dust samples from this activity. Since the material compositions in the assorted activities were consistent, the ratios derived from the solid block cutting were extrapolated to other activities, a methodology also derived from [23]. Table 3 presents the details of the TSs ratio obtained from cutting solid

blocks, focusing on PM sizes PM_{2.5} and PM₁₀. The table displays the percentage (10^{-6}) of various toxic substances (Al, Cu, Pb, Cr, Ni, Ba, As, Co, Cd, Zn) in relation to the respective PM sizes.

Table 1. PM ratios for cutting and drilling from previous studies.

Activity	PM Size	Materials (mg/m ³)				
		M20	M25	Hollow Block	Solid Block	Wood
Cutting	PM ₁	9.9	7.8	1.6	5.1	0.9
	PM _{2.5}	147.5	138.5	33.9	118.5	85.6
	PM ₁₀	5428.95	4262.51	1134.13	3538.21	483.72
Drilling	PM ₁	12.2	14.8	8.9	10.1	1.9
	PM _{2.5}	155.4	182.3	94.8	99.9	26.7
	PM ₁₀	1525.61	1714.38	1064.1	1136.7	347.32

Table 2. PM ratios for mixing, sanding, and plastering from previous studies.

Activity	PM Size	Materials (mg/m ³)		Activity	PM Size	Materials (mg/m ³)
		M20	M25			Hollow Block
Mixing	PM ₁	23.9	20.3	Plastering	PM ₁	9.3
	PM _{2.5}	508	457		PM _{2.5}	100.0
	PM ₁₀	6908	7260.0		PM ₁₀	778.0
Sanding	PM ₁	2.8	2.9			
	PM _{2.5}	42.1	50.0			
	PM ₁₀	1308.5	2134.2			

Table 3. Details of TSs ratios obtained for the solid block cutting from previous studies.

Activity	PM Size	Solid Block										
		Toxic Substance/PM (%) (10^{-6})										
		Al	Cu	Pb	Cr	Ni	Ba	As	Co	Cd	Zn	TS
Cutting	PM _{2.5}	0.0006	0.0006	0.0000	0.0000	0.0000	0.0000	0.0000	0.0000	0.0000	0.0001	0.0012
	PM ₁₀	0.0502	0.0502	0.0004	0.0001	0.0001	0.0002	0.0000	0.0001	0.0000	0.0010	0.1024

2.3. BIM Application for Health Management in Construction Project

BIM brings forth a myriad of advantages, notably in enhancing stakeholder collaboration, boosting production efficiency, and elevating revenue generation [24]. An extensive review of pertinent literature [15,24–30] underscores numerous endeavors to amalgamate various BIM functionalities for the effective management of health and safety risks. The salient benefits derived from integrating health and safety risk management within BIM frameworks are concisely summarized in Table 4. Recent years have witnessed the evolution of health and safety management systems grounded in BIM technology. These systems primarily serve to streamline the identification and communication of risk factors, significantly mitigate safety hazards for personnel, and augment overall quality, safety, and efficiency in project time and budget management.

In a parallel vein, Riaz et al. [24] developed a prototype that marries BIM with wireless sensor technology to prevent fatalities and serious injuries in confined spaces due to hazardous environmental exposures. This system utilizes Revit software version 2020 for the visualization of sensor data, allowing users to pinpoint the precise locations of sensors within a building structure. The integration of real-time sensor data with BIM emerges as a powerful application for enhancing the health and safety management of construction workers, demonstrating the potential of modern technology in mitigating occupational hazards.

Table 4. Examples of applying or developing BIM in relation to health and/or safety management.

Reference	Main Outcome or Finding	Functionality	Construction H/S Manage
[16]	Reducing personnel safety hazards	Risk scenario planning	Safety
[25]	Synthetic Images Boost Real-world Results	YOLO-v3 model	Health and Safety
[26]	Project challenge—3D/4D model technologies	3D visualization	Safety
[27]	Facilitating early risk identification and risk communication; improving construction management level	4D construction scheduling/planning	Safety
[28]	Visualization of real-time air pollution concentration monitoring and prediction of it	BIM-based sensor network module	Health
[29]	BIM platform for data-driven structural health monitoring (SHM)	SHM monitoring	SHM
[30]	Integrating planning and design of urban space and AEC projects; facilitating land-use planning, design, and management	Urban planning and design	Health and Safety

The research by Xiong and Tang [25] addresses the pressing environmental concern of dust emissions in construction sites. Recognizing the limitations of traditional methods, the researchers explore the potential of machine learning, specifically leveraging synthetic images, to improve the efficiency of monitoring processes. These images are used to train three state-of-the-art object detection algorithms: Faster-RCNN, You Only Look Once (YOLO), and Single Shot Detection (SSD). Notably, the models are trained exclusively using synthetic images, showcasing the potential of virtual environments for machine learning applications. By generating artificial data, the researchers aim to create a diverse dataset that enables robust model training. The machine learning models are designed to identify features associated with dust emissions. This innovative use of synthetic images reflects an effort to enhance the models' ability to generalize across different environmental conditions, ultimately improving the accuracy of dust emission detection in construction sites. However, it is important to consider potential limitations such as the realism of synthetic data representation and the generalizability of the model to varied construction sites scenarios.

A particularly notable contribution to HR management in the construction sector was made by Xu et al. [26]. This study expanded the scope of air pollutant monitoring through the integration of edge computing and a sensor network interface module with BIM. This innovative approach significantly enhances the capability for storing and analyzing sensor data, enabling the effective visualization of rapid changes in air pollution concentrations in real-time, along with incorporating predictive functionalities into the system. This methodology represents a groundbreaking approach to air quality monitoring and emergency management on construction sites. While Xu et al.'s research primarily emphasizes the improvement of overall site environment emergency management, it is worth highlighting that a more direct consideration of worker health in their study could have significantly enhanced the well-being and safety of the workers involved.

A thorough review of literature pertaining to the application of BIM in the construction industry underscores its increasing utilization, particularly concerning safety management in construction projects. Notably, studies [27,28] referenced in Table 4 illustrate applications such as health monitoring of structural integrity and noise distribution analysis through BIM integration. Despite these advancements, a comprehensive survey of the literature, including the seminal works listed in Table 4, indicates that the full potential of BIM in assessing and mitigating workers' health risks remains largely untapped. This gap in application is attributed to the absence of a standardized database for PM and TS. The deficiency of such a foundational dataset limits the ability to effectively leverage BIM for evaluating occupational health risks and devising appropriate preventive strategies.

3. Methodology

The authors meticulously orchestrated a series of systematically designed and feasible steps to develop a predictive system for PM and TSs, and to implement corresponding control measures through Building Information Modeling (BIM). The implemented measures, along with the information flow across each phase, are depicted in Figure 1. To construct an HRI, we utilized previously published data on PM and TS, creating a standardized database that encapsulates the HR associated with various construction activities and materials, in accordance with the USEPA HR model. For practical implementation, it was imperative that this system seamlessly integrates with the BIM model of any given construction project, highlighting HR concerns. Consequently, the authors developed a Revit-based plugin, capable of extracting the newly formulated HRI and interfacing it with the building plan, thereby enabling the delineation of HR values for specific construction activities and respective control measures. The following sections provide an in-depth description of each step in this process.

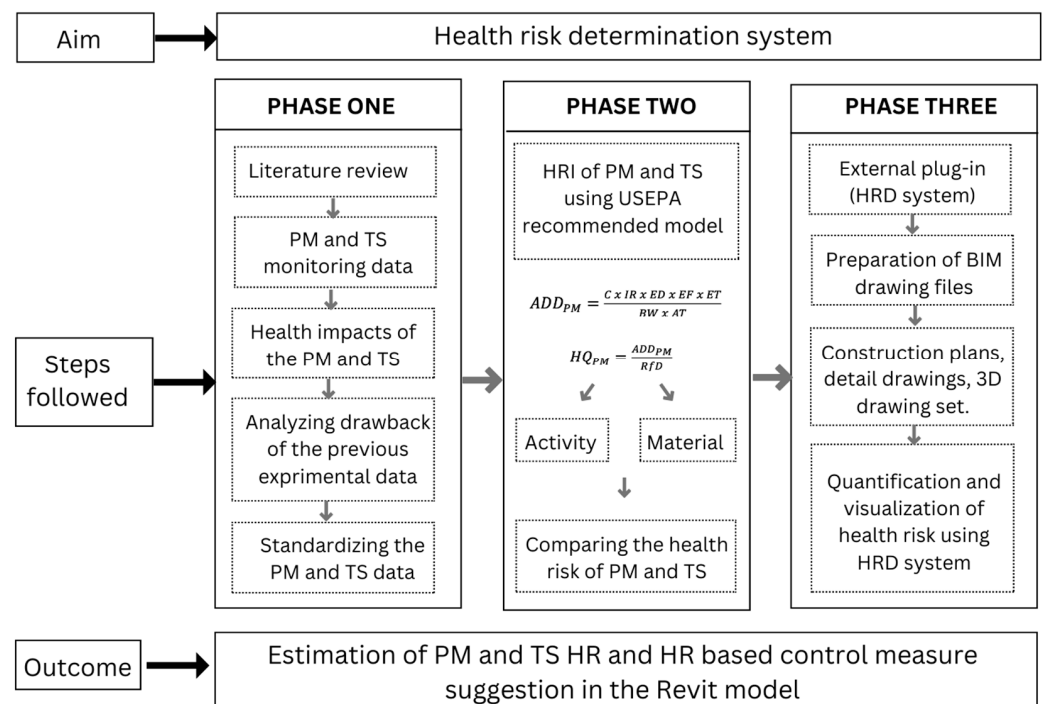


Figure 1. Schematic representation of the methodology used in this study.

3.1. Phase I—Standardization of PM and TS Experimental Data

This study rigorously evaluates the existing literature from reputable journals on HR assessments related to PM and TSs, as delineated in the literature review section. This review highlights the necessity for experimental data on PM and TSs, involving diverse materials, to be available in a standardized format to facilitate the creation of an HRI. Accordingly, this research develops a comprehensive database that includes variations in both PM and TSs, referencing [14,20]. The standardized PM and TSs data were then transformed into volumetric units (m^3). Elements or activities based on volume were adjusted to m^3 , while those based on area were converted to m^2 . For example, in drilling activities across various materials, the dimensions of the drill hole (10 mm diameter and 25.4 mm depth) were consistent, yielding a volume of $0.00797 m^3$ per hole. Given that each solid block was marked for 50 holes, the standardized PM_1 data for drilling into solid blocks was calculated as $0.160 mg/m^3$. The specific choice of drilling 50 holes in the solid block is based on several factors, including the need for a representative sample size, statistical significance, and practical considerations related to the construction activity being simulated. Moreover, each drilling event contributes a specific amount of PM_1 , and

by aggregating data from 50 holes, we can accurately assess the average mass concentration in the surrounding air. Using a standardized number of holes allows for a systematic and controlled approach, ensuring that the data collected is sufficient for analysis and generalization. This methodology was similarly employed for other activities and materials. The results of this standardization are systematically illustrated in Tables 5–8.

Table 5. The standardized data from raw data: PM emission during cutting and drilling activities.

Activity	PM Size	Materials (mg/m ³)				
		M20	M25	Hollow Block	Solid Block	Wood
Cutting	PM ₁	0.096	0.094	0.0147	0.027	0.015
	PM _{2.5}	1.435	1.669	0.3103	0.635	1.405
	PM ₁₀	52.90	51.46	10.41	19.43	7.930
Drilling	PM ₁	0.161	0.186	0.163	0.160	0.134
	PM _{2.5}	2.006	2.287	1.732	1.575	1.276
	PM ₁₀	20.20	20.35	19.38	17.93	14.22

Table 6. The standardized data from raw data: PM emission during mixing, sanding, and plastering activities.

Activity	PM Size	Materials (mg/m ³)		Activity	PM Size	Materials (mg/m ³)
		M20	M25			Hollow Block
Mixing	PM ₁	0.950	0.856	Plastering	PM ₁	0.114
	PM _{2.5}	20.18	19.10		PM _{2.5}	1.121
	PM ₁₀	277.1	304.6		PM ₁₀	11.35
Sanding	PM ₁	0.066	0.057			
	PM _{2.5}	0.998	0.987			
	PM ₁₀	31.09	42.34			

Table 7. The standardized data from raw data: TS ratio of PM emission during cutting and drilling activities.

Activity	PM Size	Materials (mg/m ³)				
		M20	M25	Hollow Block	Solid Block	Wood
Cutting	PM _{2.5}	4.1523	0.0028	0.0006	0.0012	0.0000
	PM ₁₀	0.2682	0.2789	0.0549	0.1024	0.0006
Drilling	PM _{2.5}	0.0000	0.0000	0.0000	0.0000	0.0000
	PM ₁₀	0.0001	0.0001	0.0001	0.0001	0.0000

Table 8. The standardized data from raw data: TS ratio of PM emission during mixing, sanding, and plastering activities.

Activity	PM Size	Materials (mg/m ³)		Activity	PM Size	Materials (mg/m ³)
		M20	M25			Hollow Block
Mixing	PM _{2.5}	0.0000	0.0000	Plastering	PM _{2.5}	0.0000
	PM ₁₀	0.0016	0.0015		PM ₁₀	0.0014
Sanding	PM _{2.5}	0.0000	0.0000			
	PM ₁₀	0.02	0.02			

3.2. Phase 2—PM and TS HRI

To quantify the HR associated with the standardized PM and TSs data, the methodology prescribed by the USEPA was employed. The methodology followed the USEPA

approach to transform TS concentrations and Inhalation Rates (IRs) into the Average Daily TS Exposure Dose (ADD), as prescribed by the equation provided in the USEPA guidelines [31].

In this equation, 'C' denotes the concentration of pollutants, namely PM and TS (mg/m^3), 'IR' represents the inhalation rate (m^3/h), 'ED' stands for exposure duration (years), 'ET' refers to exposure time (hours), 'EF' indicates exposure frequency (days/year), 'BW' is body weight (kg), and 'AT' signifies the average time (years). Following this, the hazard quotient for each PM category was determined using the subsequent equation as per guidelines in ref. [31].

$$ADD_{PM} = \frac{C \times IR \times ED \times EF \times ET}{BW \times AT} \quad (1)$$

Following the computation of ADD_{PM} , the hazard quotient (HQ) for each PM (HQ_{PM}) was established using the subsequent equation.

$$HQ_{PM} = \frac{ADD_{PM}}{RfD} \quad (2)$$

The term 'RfD' refers to the reference dose for non-carcinogenic substances, expressed in $\text{mg}/\text{kg} \times \text{day} (\text{d}^{-1})$ and represents the threshold dose at which adverse health effects are observed, with doses below RfD typically not associated with adverse health impacts. The RfD values employed in this study's calculations, drawn from USEPA references, vary for different types of construction dust: 0.4 for silica dust, 1.2 for cement dust, 1.6 for wood dust, and 3.2 for plaster dust [32]. In a parallel methodology, a similar approach was adopted to determine standardized TS HRI values using the aforementioned equations.

3.3. Phase 3—Health Risk Determination (HRD) BIM Plug-In System Architecture and Function

In the vanguard of innovative construction safety, this study propounds a BIM-based system named Health Risk Determination (HRD). This system seamlessly integrates the USEPA calculation method incorporating the authors' suggested standardized HRI values for PM and TSs within BIM. This heralds a transformative era in mitigating HRs for workers involved in construction projects. This section provides a comprehensive overview of the system architecture and functionalities of the HRD system. The process map is stated in Figure 2.

The very essence of the HRD system lies in its meticulously designed system architecture. The choice of Visual Studio.Net as a development platform was made, which permits programming within Revit using Revit Application Programming Interface (API). This interface acts as the communication bridge, enabling HRD to dynamically interface with the voluminous data and complex elements within the BIM model. HRD operates through a self-updating graphical user interface (GUI), as a Revit plug-in. This external application integrates into the Revit software, serving as the portal through which users interact with the functionalities of HRD. The C# programming language was chosen as the coding language. The coding intricacies reflect a commitment to precision, ensuring that the HRD's algorithms operate with a quantitative framework deeply rooted in the methodologies advocated by the USEPA (refer to Section 3.2). HRD adeptly leverages this framework, ensuring that calculations adhere to its standards.

Recognizing the importance of user-friendly guidance, HRD incorporates an interaction that ensures that stakeholders, irrespective of technical proficiency, can navigate HRD with confidence. The plugin's interface begins with an installation process onto major BIM platforms (Revit) ensuring accessibility across the construction industry. Upon launching the HRD plugin, users are guided to input relevant volume data and choose materials of a designated element from the BIM model necessitating subsequent calculation. Further, the system architecture plays a pivotal role in empowering the plugin to conduct HR calculations within the model. The integration of this database allows for a detailed

and accurate representation of HR factors associated with specific construction activity and materials, enhancing the overall efficacy of the HRD system.

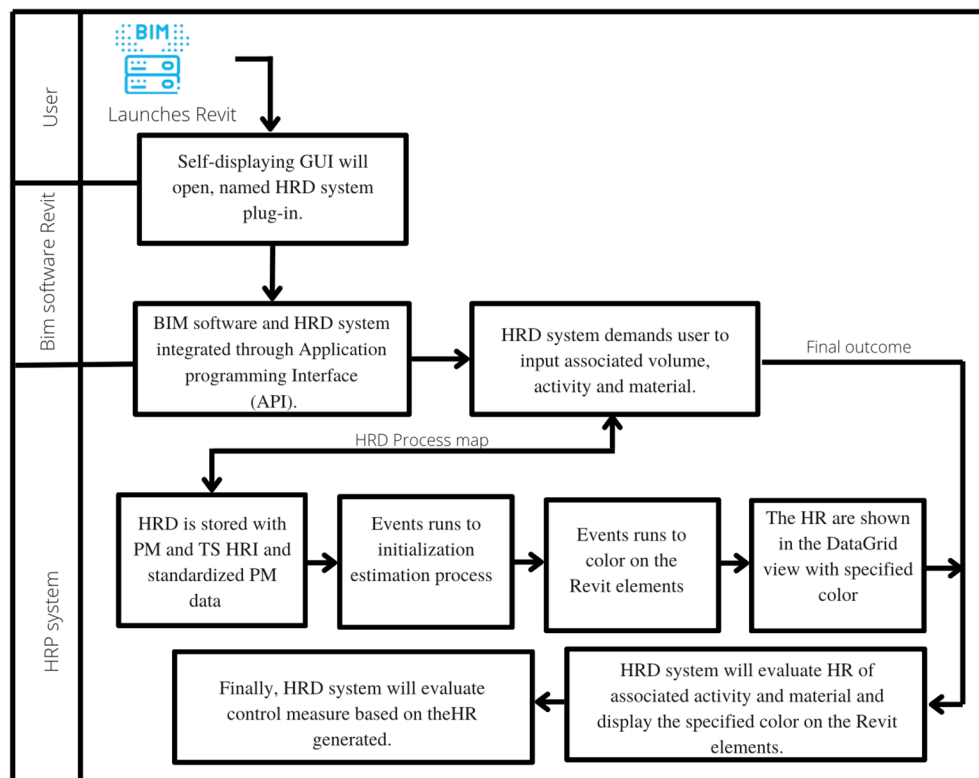


Figure 2. Process map of the HRD system.

Following the intricate calculations within the HRD system, a series of consequential actions are set to enhance HR management in construction projects. Within the BIM model, HR assessments are visually conveyed through a sophisticated color-coded system. Specific color filters and coding correspond to different risk levels, providing a visual representation of the HR associated with each element.

The quantified HR within the BIM model is visualized using a color-coded system. Specific color filters and coding are established to correspond with different risk levels, allowing for the application of parameters based on the value of the risk. The color associated with a building element reflects the calculated HR. Additionally, the HRD system implements tailored control measures on elements, guided by the severity of the calculated HR. Facilitating this process involves the integration of a specialized control measure library directly into the BIM model. BIM's inherent capability to incorporate both the geometry and semantics of building components plays a pivotal role. Semantics in BIM enhance the 3D building model by specifying the properties and attributes of each building component [33]. This integration is achieved through the creation of URL-type parameters linked with individual BIM elements, empowering the HRD system to seamlessly associate essential HR information with each specific element.

4. HRI Analysis and Results

In quantifying the HRI for PM and TSs, the authors meticulously applied the USEPA methodology as detailed in Section 3.2. This analytical approach allows us to discern the HR associated with PM and TS exposure. The corresponding findings are elucidated in Tables 9 and 10 for PM and TSs, respectively. The risk level assessment adhered to USEPA guidelines: HR values below 10^{-6} are considered acceptable and safe, values between 10^{-4} and 10^{-6} suggest a potential HR, and values above 10^{-4} indicate a severe HR [32]. The highest HR during drilling was recorded in PM₁₀ for the M25 cement block

(1.4×10^{-6} mg/m³), followed by the M20 cement block (1.1×10^{-6} mg/m³) and solid block (1.3×10^{-6} mg/m³). The lowest HR in PM₁₀ was observed while drilling wood (7.6×10^{-12} mg/m³). However, the TS HRI exhibited a different pattern, with all activities showing medium risk levels, ranging from 9.6×10^{-5} mg/m³ in M20 PM₁₀ to 8.3×10^{-6} mg/m³ in hollow block PM_{2.5}.

Table 9. Details of PM HRI. (Low-HR, Medium-HR).

PM HRI (mg/m ³)									
Activity	Material	PM Size	HR	Activity	Material	PM Size	HR		
Cutting	Concrete block M20	PM ₁	4.4×10^{-9}	Drilling	Concrete block M20	PM ₁	9.1×10^{-9}		
		PM _{2.5}	6.5×10^{-8}			PM _{2.5}	1.1×10^{-7}		
		PM ₁₀	2.4×10^{-6}			PM ₁₀	1.1×10^{-6}		
	Concrete block M25	PM ₁	4.8×10^{-9}		Concrete block M25	PM ₁	1.6×10^{-7}		
		PM _{2.5}	8.5×10^{-8}			PM _{2.5}	1.6×10^{-7}		
		PM ₁₀	2.6×10^{-6}			PM ₁₀	1.4×10^{-6}		
	Hollow block	PM ₁	0.9×10^{-10}		Hollow block	PM ₁	1.2×10^{-8}		
			PM _{2.5}				1.8×10^{-8}	PM _{2.5}	1.2×10^{-7}
			PM ₁₀				6.3×10^{-7}	PM ₁₀	1.4×10^{-6}
		Solid block	PM ₁			1.5×10^{-9}	Solid block	PM ₁	1.2×10^{-8}
			PM _{2.5}			3.4×10^{-8}		PM _{2.5}	1.2×10^{-7}
			PM ₁₀			1.0×10^{-6}		PM ₁₀	1.3×10^{-6}
Wood	PM ₁	5.3×10^{-8}	Wood	PM ₁	7.6×10^{-8}				
	PM _{2.5}	4.6×10^{-6}		PM _{2.5}	7.6×10^{-7}				
	PM ₁₀	6.7×10^{-5}		PM ₁₀	7.6×10^{-12}				
Mixing	Concrete block M20	PM ₁	5.1×10^{-8}	Sanding	Concrete block M20	PM ₁	3.6×10^{-9}		
		PM _{2.5}	1.0×10^{-6}			PM _{2.5}	5.4×10^{-8}		
		PM ₁₀	1.5×10^{-5}			PM ₁₀	1.6×10^{-6}		
	Concrete block M25	PM ₁	4.5×10^{-8}		Concrete block M25	PM ₁	3.6×10^{-9}		
		PM _{2.5}	1.0×10^{-6}			PM _{2.5}	5.4×10^{-8}		
Plastering	Hollow block	PM ₁	1.0×10^{-8}	Hollow block	PM ₁	1.6×10^{-6}			
		PM _{2.5}	1.1×10^{-7}		PM _{2.5}	5.4×10^{-8}			
		PM ₁₀	8.3×10^{-7}		PM ₁₀	1.6×10^{-6}			

Table 10. Details of TS HRI. (Medium-HR, High-HR).

TS HRI (mg/m ³)									
Activity	Material	PM Size	HR	Activity	Material	PM Size	HR		
Cutting	Concrete block M20	PM _{2.5}	4.2×10^{-6}	Drilling	Concrete block M20	PM _{2.5}	7.4×10^{-6}		
		PM ₁₀	1.5×10^{-4}			PM ₁₀	7.5×10^{-5}		
	Concrete block M25	PM _{2.5}	5.5×10^{-5}		Concrete block M25	PM _{2.5}	1.0×10^{-5}		
		PM ₁₀	1.7×10^{-3}			PM ₁₀	9.6×10^{-5}		
	Hollow block	PM _{2.5}	1.2×10^{-6}		Hollow block	PM _{2.5}	8.3×10^{-6}		
		PM ₁₀	4.1×10^{-5}			PM ₁₀	9.3×10^{-5}		
	Solid block	PM _{2.5}	2.2×10^{-5}		Solid block	PM _{2.5}	7.9×10^{-5}		
		PM ₁₀	7.0×10^{-5}			PM ₁₀	9.0×10^{-5}		
	Wood	PM _{2.5}	4.5×10^{-5}		Wood	PM _{2.5}	4.5×10^{-6}		
		PM ₁₀	5.4×10^{-6}			PM ₁₀	5.4×10^{-5}		
	Mixing	Concrete block M20	PM _{2.5}		7.1×10^{-5}	Sanding	Concrete block M20	PM _{2.5}	3.5×10^{-6}
			PM ₁₀		9.8×10^{-4}			PM ₁₀	1.1×10^{-4}
Concrete block M25		PM _{2.5}	6.7×10^{-5}	Concrete block M25	PM _{2.5}		3.4×10^{-6}		
		PM ₁₀	1.0×10^{-3}		PM ₁₀		1.4×10^{-4}		
Plastering	Hollow Block	PM _{2.5}	7.4×10^{-6}	Hollow Block	PM _{2.5}	7.4×10^{-6}			
		PM ₁₀	5.4×10^{-5}		PM ₁₀	5.4×10^{-5}			

Similarly, during cutting activities, PM HR levels mirrored those in drilling, with the highest and lowest HRs observed in PM₁₀ at 6.7×10^{-5} mg/m³ and PM₁ at 0.9×10^{-10} mg/m³, respectively, when cutting wood and hollow block. The highest TS HR was seen in M20 PM₁₀ at 1.5×10^{-3} mg/m³, and the lowest in wood PM₁₀ at

$5.4 \times 10^{-6} \text{ mg/m}^3$. Sanding M20 and M25 cement blocks in PM_{10} showed the highest HRs at $1.6 \times 10^{-6} \text{ mg/m}^3$ and $2.2 \times 10^{-6} \text{ mg/m}^3$, respectively, while the lowest in PM_1 was for M20 at $3.1 \times 10^{-9} \text{ mg/m}^3$.

The TS HR for sanding activities indicated a medium-risk level across all activities, ranging from $1.4 \times 10^{-4} \text{ mg/m}^3$ to $3.5 \times 10^{-6} \text{ mg/m}^3$. Mixing activities yielded HR values of $1.6 \times 10^{-5} \text{ mg/m}^3$ and $4.5 \times 10^{-8} \text{ mg/m}^3$. The highest TS HR in PM_{10} for M20 cement block was $1.0 \times 10^{-3} \text{ mg/m}^3$, and the lowest in $\text{PM}_{2.5}$ for M20 was $7.1 \times 10^{-5} \text{ mg/m}^3$. Plastering activities indicated low PM HR levels, ranging from $1.1 \times 10^{-7} \text{ mg/m}^3$ to $1.0 \times 10^{-8} \text{ mg/m}^3$. The overall HR for the cutting of an M25 cement block in PM_{10} was the highest at $4.1 \times 10^{-3} \text{ mg/m}^3$, whereas the lowest in $\text{PM}_{2.5}$ for drilling a hollow block was $8.3 \times 10^{-6} \text{ mg/m}^3$. Consistent results were observed for the TS HR in cutting wood in $\text{PM}_{2.5}$ ($4.5 \times 10^{-5} \text{ mg/m}^3$) and PM_{10} ($5.4 \times 10^{-6} \text{ mg/m}^3$), showing a minor difference from drilling wood in $\text{PM}_{2.5}$ ($4.5 \times 10^{-6} \text{ mg/m}^3$) and PM_{10} ($5.4 \times 10^{-5} \text{ mg/m}^3$). The most significant difference was noted in mixing M25 for PM_{10} and sanding M25 cement block for PM_{10} . The findings indicate that TS HR is higher than PM in all activities and materials, with PM values being 65 times lower than TS. While HR assessments have traditionally emphasized PM, the HRI demonstrates that control measures should also consider TS.

The highest PM HR recorded across all activities was during the cutting of the M20 cement block for PM_{10} , registering at $2.4 \times 10^{-6} \text{ mg/m}^3$. Conversely, the lowest PM HR was observed during the cutting of hollow blocks ($0.9 \times 10^{-10} \text{ mg/m}^3$), which was 3.6 times lower than the highest PM risk level. PM risk levels for PM_{10} , $\text{PM}_{2.5}$, and PM_1 during hollow block drilling were found to be 5% lower compared to those during solid block drilling. The risk level values for PM_{10} , $\text{PM}_{2.5}$, and PM_1 in the drilling of M20 and M25 cement blocks were $9.1 \times 10^{-9} \text{ mg/m}^3$, $1.1 \times 10^{-7} \text{ mg/m}^3$, $1.1 \times 10^{-6} \text{ mg/m}^3$, and $1.6 \times 10^{-7} \text{ mg/m}^3$, $1.6 \times 10^{-7} \text{ mg/m}^3$, $1.4 \times 10^{-6} \text{ mg/m}^3$, respectively, showing a variance of 6.8%. Despite the relatively small 5% difference in PM concentrations between hollow block and solid block drilling, cutting the same materials displayed significant variations in PM concentrations.

PM HR values for cutting solid blocks were 10% higher than those for cutting hollow blocks. A similar trend was observed in PM risk values from cutting M20 and M25 cement blocks, mirroring the drilling activity patterns. Notably, PM risk levels during the sanding of M25 cement blocks were 9% higher than those for M20 cement blocks. These findings underscore that the HR associated with PM and TSs varies depending on the materials used in construction activities. The results indicate that higher-density materials, such as the M25 cement block, exhibit a higher HR, whereas lower-density materials like wood present a lower HR.

5. Illustrative Case Example

5.1. Project Information

This illustrative case study is designed to validate the applicability of the HRD system. The study integrates the HRI determination process into the realm of BIM. This integration is expertly facilitated by the advanced functionalities encapsulated within the HRD plugin. The library building renovation project was chosen for this case study, due to the intrinsic challenges associated with renovation works that involve diverse materials and activities. Moreover, renovation projects inherently introduce a multitude of indoor air pollutants into the environment, including PM, heavy metals, fibrous materials, various gaseous emissions, and a spectrum of organic compounds [3].

This case study focuses on the renovation of a 300,000-square-foot library spanning five floors. The project, unfolding over one week, includes diverse tasks such as selective demolition, plumbing, masonry work, and electrical installations across the second to fourth floors. The principal activities of the renovation involve comprehensive structural modifications and upgrades, including the dismantling and reinstallation of windows, doors, and tiling, the revamping of bathroom fixtures like sinks and toilets, and the artistic enhancement of the interior through painting and wall treatments. These broad renovation

activities are further subdivided into tasks such as cutting, sanding, mixing, drilling, and plastering. Various materials like concrete (M20 and M25 grades), building blocks, and wood are employed. This setting provides a detailed context for evaluating the HRD system's application in a complex remodeling scenario.

5.2. Application of the HRD System

The HRD system's workflow is visually outlined in Figure 3, providing a clear overview of the system. To initiate the process, the construction supervisor relies on a combination of resources, including the detailed remodeling work schedule and 2D or 3D BIM drawings. In the practical application of the HRD system, the site supervisor also begins the process by depending on the aforementioned resources. These resources offer crucial insights into upcoming activities, allowing the supervisor to identify specific areas of focus and understand the materials and volume involved (Figure 3a). Furthermore, the supervisor utilizes a specially designed external plugin called the HRD within Revit, developed as a part of this research endeavor. The HR assessment of each daily activity and sub-task can be calculated with the available schedule, materials, and volume (Figure 3b).

The supervisor gains the ability to evaluate the HR values associated with the day's construction activities and materials (Figure 3d) by leveraging the plugin's functionalities (Figure 3c). Armed with this valuable information, the supervisor can make informed decisions and implement control measures as needed to ensure the safety and well-being of the workers (Figure 3e).

The HRD system's implementation in construction activities is meticulously detailed in Figure 3, showcasing its integral role in task management. To precisely calculate the HR for specific construction activities, the process begins with a comprehensive analysis of work orders, breaking down each activity into its tasks. For example, the door removal activity is methodically segmented into distinct phases: firstly, drilling out the hinges, followed by chipping out the frame, then removing the lintel, and finally, cleaning the surface. In the task of door removal, the procedure diverges slightly, adhering closely to the detailed drawing of the door as illustrated in Figure 3b.

The HR calculation, as delineated in the methodology section, is a critical component of this system. Emphasizing accuracy and detail, Table 8 in the report presents the outcomes derived from the HRD system. The system's plugin, a pivotal element in this framework, archives the HRI and control measures data, corresponding to varying HR levels. Consequently, the BIM model highlights these elements, showcasing the estimated HR levels in a visually intuitive manner. For example, the HR for the initial task of drilling out the hinges is categorized as low (referenced in Table 11), prompting the HRD system to color-code the hinges in blue and recommend the usage of personal protective equipment (PPE) as a preventive measure. This color-coding and recommendation process is an innovative approach to ensuring safety and efficiency in construction activities.

Table 11. Removing of door activity results estimated by the HRD system (work progress).

Activity ID	Activity Title	Start Date	Due Date	Duration (Days)	Week 1				
					M	T	W	Th	F
1	Remove windows and doors (2nd, 3rd, and 4th floor)	3 October 2021	3 November 2021	2					
1.1	Room1	3 October 2021	3 November 2021	2					
		PM ₁	PM _{2.5}	PM ₁₀		TS _{2.5}		TS ₁₀	
Task	1.1.1 Drilling out the hinges	3.1×10^{-12}	3.7×10^{-11}	3.7×10^{-10}	1.4×10^{-9}			5.6×10^{-8}	
	1.1.2 Chipping out the frames	4.6×10^{-11}	8.2×10^{-10}	2.5×10^{-8}	4.0×10^{-8}			1.4×10^{-6}	
	1.1.3 Removing of lintel	3.1×10^{-11}	5.5×10^{-10}	1.6×10^{-8}	2.7×10^{-8}			9.7×10^{-7}	

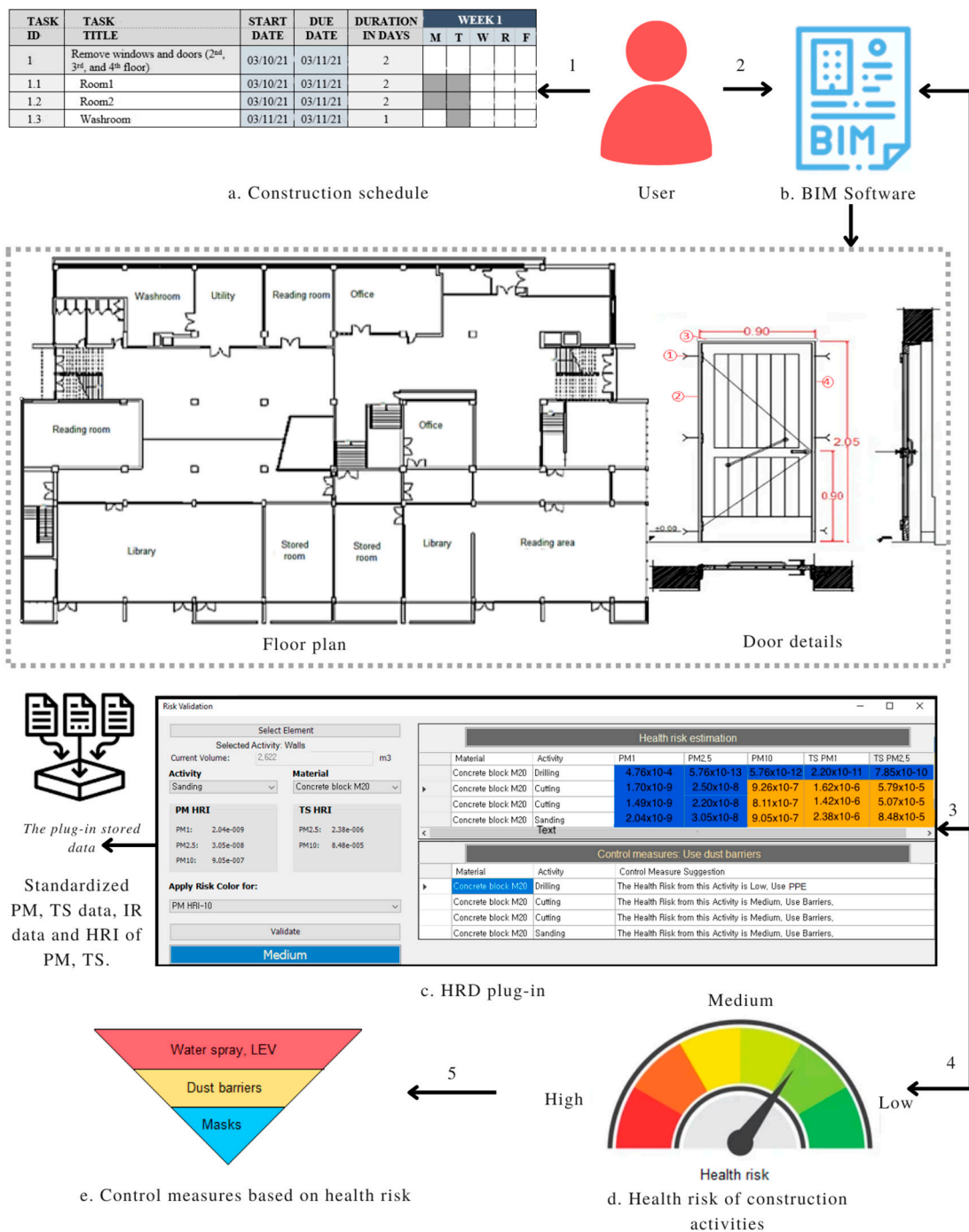


Figure 3. Flow chart of HRD system from a user’s perspective.

5.3. Case Study Results and Discussion

The case study, set in the context of a library building earmarked for remodeling, serves as a hypothetical yet insightful exploration into the capabilities of the HRD system. Within this framework, the daily PM and TS HR levels, emanating from diverse construction activities, were meticulously calculated using the HRP system. Medium HR levels warrant the installation of dust barriers [34] whereas low HR levels are deemed safe without additional control measures. Notably, the results from the door activity estimation indicate the necessity for dust barriers during the door removal process.

Contrasting with the conventional HR estimation process, which requires manual input of multiple variables (PM, IR, ED, ET, EF, BW, AT) derived from construction activities and

workers' data, the HRD system introduces a paradigm shift. The conventional approach, often laborious and time-consuming, applies continuous control measures indiscriminately across the construction site. In stark contrast, the semi-automated HRD system leverages 2D or 3D Revit construction drawings and the specialized HRD plugin to quantify HR more efficiently. Consequently, site supervisors can rapidly implement control measures that are finely tuned to address high-risk activities, as evidenced by the case study results. This targeted approach not only quantifies HRs at the level of individual activities but also empowers supervisors to promptly adopt control measures for high-risk scenarios.

This study casts a new light on the assessment of HRs at the activity and material level in the construction industry. By visualizing the HR associated with daily construction activities, health managers can proactively implement adequate control measures onsite. This innovative system not only aids in current health risk management but also provides a valuable tool for future researchers to predict and mitigate occupational health impairments in the construction industry.

As such, the HRD system was built based on the concept that was first attempted, but it is necessary to continue to build PM and TS data based on various types of work, materials, and construction methods, and additional research efforts are needed to allow the BIM-based HRD system to settle in the work process.

6. Conclusions

This study underscores the pressing issue of health impairments among construction workers, primarily stemming from exposure to PM and TS particles. The systematic methodology introduced a quantitative approach to assess the HR associated with activities with high PM emissions. Drawing upon PM and TS simulation data from previously published articles, the authors meticulously prepared a standardized HRI by transforming them into a standardized format, thus enhancing its applicability and scalability for use in various construction projects.

In contrast to prior investigations, notably the study conducted by Choi et al. [14], which utilized raw data rendering it unsuitability for standardized calculations, the present research represents a notable advancement. While the prior study offered valuable insights using raw data, our current research takes a substantial leap forward by addressing this limitation. We introduce a systematic methodology that standardizes raw PM and TS data to create an HRI, thereby enhancing its applicability and scalability. Furthermore, we have developed a specialized HRD system plugin for Revit, which allows the integration of HRI data with BIM, facilitating the quantification of HR at the activity level within the BIM environment.

The illustrative case study within this article clearly demonstrates the efficacy of the BIM-integrated HRD system in estimating HR from specific construction activities. Construction managers can now review HR metrics within Revit alongside ongoing work processes and implement the recommended control measures. This capability not only aids in visualizing but also in mitigating the health impacts to construction workers on construction sites. By enabling the estimation of HR at the activity level, the system empowers health and safety teams to preemptively prepare and implement appropriate control measures.

The findings of this study illuminate the pathway for activity and material-level HR assessment within the construction industry. Experts in the academia–industry field of construction should pay attention to the significant contributions this study has made, which are unprecedented from the perspective of the construction industry. Firstly, the quantification of the health risk of PM and TSs and their integration into work processes, and secondly, the expansion of BIM's adaptability into the field of health and safety management, demonstrating its potential applicability across various construction trades. However, it is important to note that the current system relies on a standard database, which, while comprehensive, is limited to certain construction materials and work practices. Therefore, there is a crucial need to expand this database progressively, incorporating

a wider array of activities, materials, and equipment to enhance its applicability and effectiveness across diverse construction scenarios.

Author Contributions: Conceptualization, D.C. and J.-H.C.; Methodology, A.J., D.C. and J.-H.C.; Formal analysis, A.J.; Writing—original draft, A.J. and D.C.; Writing—review & editing, D.C. and J.-H.C.; Visualization, A.J., D.C. and J.-H.C.; Supervision, J.-H.C.; Funding acquisition, J.-H.C. All authors have read and agreed to the published version of the manuscript.

Funding: This work is supported by the Korea Agency for Infrastructure Technology Advancement (KAIA) grant funded by the Ministry of Land, Infrastructure and Transport (National Research for Smart Construction Technology: Grant 225MIP-A156381-03), and the Basic Science Research Program through the National Research Foundation of Korea (NRF) funded by the Ministry of Education (2022R111A3073717).

Data Availability Statement: Data available on request from the authors. The raw data supporting the conclusions of this article will be made available by the authors on request.

Conflicts of Interest: The authors declare no conflict of interest.

References

1. Apte, J.S.; Brauer, M.; Cohen, A.J.; Ezzati, M.; Pope, C.A., III. Ambient PM_{2.5} Reduces Global and Regional Life Expectancy. *Environ. Sci. Technol. Lett.* **2018**, *5*, 546–551. [CrossRef]
2. Brook, R.D.; Franklin, B.; Cascio, W.; Hong, Y.; Howard, G.; Lipsett, M.; Luepker, R.; Mittleman, M.; Samet, J.; Smith, S.C.; et al. Air Pollution and Cardiovascular Disease. *Circulation* **2004**, *109*, 2655–2671. [CrossRef] [PubMed]
3. Environmental Protection Agency. *EPA Risk Assessment Guidance for Superfund. Volume I Human Health Evaluation Manual (Part A)*; Environmental Protection Agency: Washington, DC, USA, 1989; Volume I, p. 289. Available online: <https://www.epa.gov/risk/risk-assessment-guidance-superfund-rags-part> (accessed on 11 November 2023).
4. Yang, H.; Song, X.; Zhang, Q. RS&GIS Based PM Emission Inventories of Dust Sources over a Provincial Scale: A Case Study of Henan Province, Central China. *Atmos. Environ.* **2020**, *225*, 117361. [CrossRef]
5. Latif, M.T.; Baharudin, N.H.; Velayutham, P.; Awang, N.; Hamdan, H.; Mohamad, R.; Mokhtar, M.B. Composition of Heavy Metals and Airborne Fibers in the Indoor Environment of a Building during Renovation. *Environ. Monit. Assess.* **2011**, *181*, 479–489. [CrossRef] [PubMed]
6. Li, H.; Fang, C.H.Y.; Shi, W.; Gurusamy, S.; Li, S.; Krishnan, M.N.; George, S. Size and Site Dependent Biological Hazard Potential of Particulate Matters Collected from Different Heights at the Vicinity of a Building Construction. *Toxicol. Lett.* **2015**, *238*, 20–29. [CrossRef] [PubMed]
7. Azarmi, F.; Kumar, P.; Mulheron, M. The Exposure to Coarse, Fine and Ultrafine Particle Emissions from Concrete Mixing, Drilling and Cutting Activities. *J. Hazard. Mater.* **2014**, *279*, 268–279. [CrossRef] [PubMed]
8. Klotz, K.; Weistenhöfer, W.; Neff, F.; Hartwig, A.; Van Thriel, C.; Drexler, H. The Health Effects of Aluminum Exposure. *Dtsch. Aerzteblatt Int.* **2017**, *114*, 653–659. [CrossRef]
9. Wang, G.; Zhang, L.; Zhang, J. A Review of Electrode Materials for Electrochemical Supercapacitors. *Chem. Soc. Rev.* **2012**, *41*, 797–828. [CrossRef]
10. Zhao, H.; Xia, B.; Fan, C.; Zhao, P.; Shen, S. Human Health Risk from Soil Heavy Metal Contamination under Different Land Uses near Dabaoshan Mine, Southern China. *Sci. Total Environ.* **2012**, *417–418*, 45–54. [CrossRef]
11. Muleski, G.E.; Cowherd, C.; Kinsey, J.S. Particulate Emissions from Construction Activities. *J. Air Waste Manag. Assoc.* **2005**, *55*, 772–783. [CrossRef]
12. Cheriyan, D.; Choi, J. Estimation of Particulate Matter Exposure to Construction Workers Using Low-Cost Dust Sensors. *Sustain. Cities Soc.* **2020**, *59*, 102197. [CrossRef]
13. Cheriyan, D.; Khamraev, K.; Choi, J. Varying Health Risks of Respirable and Fine Particles from Construction Works. *Sustain. Cities Soc.* **2021**, *72*, 103016. [CrossRef]
14. Choi, J.; Khamraev, K.; Cheriyan, D. Hybrid Health Risk Assessment Model Using Real-Time Particulate Matter, Biometrics, and Benchmark Device. *J. Clean. Prod.* **2022**, *350*, 131443. [CrossRef]
15. Barazzetti, L.; Banfi, F.; Brumana, R.; Previtali, M. Creation of Parametric BIM Objects from Point Clouds Using Nurbs. *Photogramm. Rec.* **2015**, *30*, 339–362. [CrossRef]
16. Salman, A. Building Information Modeling (BIM): Trends, Benefits, Risks, and Challenges for the AEC Industry. *Leadersh. Manag. Eng.* **2011**, *11*, 241–252. [CrossRef]
17. World Health Organization. *Health Effects of Particulate Matter: Policy Implications for Countries in Eastern Europe, Caucasus and Central Asia*; World Health Organization, Regional Office for Europe: Copenhagen, Denmark, 2013; ISBN 9789289000017.
18. de Moraes, R.J.B.; Bastos, C.D.; Silva, A.I.P. Particulate Matter Concentration from Construction Sites: Concrete and Masonry Works. *J. Environ. Eng.* **2016**, *142*, 5016004. [CrossRef]

19. Tong, R.; Cheng, M.; Zhang, L.; Liu, M.; Yang, X.; Li, X.; Yin, W. The Construction Dust-Induced Occupational Health Risk Using Monte-Carlo Simulation. *J. Clean. Prod.* **2018**, *184*, 598–608. [[CrossRef](#)]
20. Cheriyan, D.; Hyun, K.Y.; Jaegoo, H.; Choi, J. Assessing the Distributional Characteristics of PM₁₀, PM_{2.5}, and PM₁ Exposure Profile Produced and Propagated from a Construction Activity. *J. Clean. Prod.* **2020**, *276*, 124335. [[CrossRef](#)]
21. Khamraev, K.; Cheriyan, D.; Choi, J. A Review on Health Risk Assessment of PM in the Construction Industry—Current Situation and Future Directions. *Sci. Total Environ.* **2021**, *758*, 143716. [[CrossRef](#)]
22. Baldauf, R.W.; Lane, D.D.; Marotz, G.A.; Wiener, R.W. Performance Evaluation of the Portable MiniVOL Particulate Matter Sampler. *Atmos. Environ.* **2001**, *35*, 6087–6091. [[CrossRef](#)]
23. Núñez, J.; Wang, Y.; Bäumer, S.; Boersma, A. Inline Infrared Chemical Identification of Particulate Matter. *Sensors* **2020**, *20*, 4193. [[CrossRef](#)] [[PubMed](#)]
24. Riaz, Z.; Arslan, M.; Kiani, A.K.; Azhar, S. CoSMoS: A BIM and Wireless Sensor Based Integrated Solution for Worker Safety in Confined Spaces. *Autom. Constr.* **2014**, *45*, 96–106. [[CrossRef](#)]
25. Xiong, R.; Tang, P. Machine learning using synthetic images for detecting dust emissions on construction sites. *Smart Sustain. Built Environ.* **2021**, *10*, 487–503. [[CrossRef](#)]
26. Xu, Z.; Ran, Y.; Rao, Z. Design and Integration of Air Pollutants Monitoring System for Emergency Management in Construction Site Based on BIM and Edge Computing. *Build. Environ.* **2022**, *211*, 108725. [[CrossRef](#)]
27. Li, X.; Xiao, Y.; Guo, H.; Zhang, J. A BIM Based Approach for Structural Health Monitoring of Bridges. *KSCE J. Civ. Eng.* **2022**, *26*, 155–165. [[CrossRef](#)]
28. Weile, W.; Chao, W.; Yongcheol, L. BIM-Based Construction Noise Hazard Prediction and Visualization for Occupational Safety and Health Awareness Improvement. *Comput. Civ. Eng.* **2017**, *2017*, 262–269.
29. Kim, K.; Cho, Y.; Zhang, S. Integrating Work Sequences and Temporary Structures into Safety Planning: Automated Scaffolding-Related Safety Hazard Identification and Prevention in BIM. *Autom. Constr.* **2016**, *70*, 128–142. [[CrossRef](#)]
30. Jaiswal, A.S. An Overview of Building Information Modeling (BIM) & Construction of 4D BIM Model. *Int. J. Res. Appl. Sci. Eng. Technol.* **2021**, *9*, 3754–3758. [[CrossRef](#)]
31. US Environmental Protection Agency. *Exposure Factors Handbook: 2011 Edition*; EPA/600/R-09/052F; US Environmental Protection Agency: Washington, DC, USA, 2011; pp. 1–1466.
32. United States Environmental Protection Agency. *Wildlife Exposure Factors Handbook*; EPA 600-R-93-187; United States Environmental Protection Agency: Washington, DC, USA, 1993; Volume I, p. 572.
33. Liao, W.-B.; Ju, K.; Zhou, Q.; Gao, Y.-M.; Pan, J. Forecasting PM_{2.5} Induced Lung Cancer Mortality and Morbidity at County-Level in China Using Satellite-Derived PM_{2.5} Data from 1998 to 2016: A Modelling Study. *Lancet* **2019**, *394*, S70. [[CrossRef](#)]
34. Simmons, C.E.; Jones, R.M.; Boelter, F.W. Factors Influencing Dust Exposure: Finishing Activities in Drywall Construction. *J. Occup. Environ. Hyg.* **2011**, *8*, 324–336. [[CrossRef](#)]

Disclaimer/Publisher’s Note: The statements, opinions and data contained in all publications are solely those of the individual author(s) and contributor(s) and not of MDPI and/or the editor(s). MDPI and/or the editor(s) disclaim responsibility for any injury to people or property resulting from any ideas, methods, instructions or products referred to in the content.